
PERGAMON

Journal of the Mechanics and Physics of Solids
48 (2000) 1175–1201

JOURNAL OF THE
MECHANICS AND
PHYSICS OF SOLIDS

www.elsevier.com/locate/jmps

Numerical simulation of martensitic transformations in two- and three-dimensional polycrystals

Oscar P. Bruno*, Guillermo H. Goldsztein

California Institute of Technology, Department of Applied Mathematics, Caltech, Pasadena, CA 91125, USA

Received 19 January 1999; received in revised form 16 July 1999

Abstract

We introduce a fast numerical method for the evaluation of the effective elastic energy in martensitic polycrystals in two and three dimensions. The overall complexity of the method is $\mathcal{O}(N)$ operations, where N is the number of component crystallites. Upper and lower bounds on the energy are also presented which allow us to estimate the accuracy of the numerical results. Our new three-dimensional computations and bounds for random polycrystals, which are the first ones available in the literature, provide substantial insights on the behavior of polycrystalline martensites. They suggest that recoverable strains can be much larger than those attainable with zero energy.

Keywords: Polycrystal; Martensite; Phase transitions; Homogenization; Plasticity

1. Introduction

We present a fast method for the evaluation of overall elastic energies in two- and three-dimensional martensitic polycrystals. The basic component of our method is an explicit solution for Eshelby-type problems on cubic elements. Fast

* Corresponding author.

0022-5096/00/$ - see front matter
PII: S0022-5096(99)00074-5

computation of the polycrystal energy results through a rapidly convergent sequence of approximations which can, in fact, be interpreted as a generalization of a class of upper bounds introduced recently. The overall complexity of the method is $\mathcal{O}(N)$ operations, where N is the number of component crystallites. We also present lower and upper bounds for the energy, giving additional insights on the microscopic phenomena leading to the observed structural behavior. In particular we establish that, for random polycrystals with cubic to orthorhombic basic transformation strains, the overall energy increases cubically with the departure from the zero energy set. Thus, large deformations can be accommodated with very small energies, suggesting that applied strains would be recoverable well beyond the zero energy set.

This paper is organized as follows:

In Section 2, we describe the polycrystals we consider and we derive a variety of useful expressions for the effective energy. In Section 3 we describe our numerical method, which is based on a convergent sequence of approximations of the effective energy. In Section 4 we derive rigorous upper and lower bounds for a class of model polycrystals. We conclude in Section 5, where we present our numerical results and discuss different features of the effective energy and its bounds.

2. Overall elastic energy

2.1. Microgeometry, transformations and elastic properties

We consider two- and three-dimensional polycrystals $\mathscr{P}$, consisting of a collection of grains or crystallites G

$$\mathscr{P} = \bigcup_{G \in G} G.$$

The crystallographic orientation of a grain G is given by a proper rotation $R = R(G)$. We take both grains and orientations to be random variables and we assume that their corresponding statistical distributions are spatially homogeneous, as described in Bruno et al. (1996).

Each grain can undergo a shape deforming phase transition leading to associated deformations or transformation strains. The possible transformation strains of a single crystal depend on the orientation of the underlying crystalline lattice. More precisely, a single crystal whose orientation is given by a certain rotation R of the reference crystal will exhibit transformation strains equal to rotated versions, by the same rotation R, of those corresponding to the reference configuration. Thus calling

$$\varepsilon^{\mathrm{T}(0)} = 0, \varepsilon^{\mathrm{T}(1)}, \ldots, \varepsilon^{\mathrm{T}(k)}$$

the basic transformation strains (or variants) in a reference single crystal, the corresponding variants in a rotated single crystal, with rotation matrix R, are given by $R\varepsilon^{\mathrm{T}(i)}R^{\mathrm{T}}$.

Most often, fine laminated microstructures are found as the form in which the phase transition takes place within individual grains; in many cases, further, the full sub-granular microstructure consists of a single fine laminate, perhaps of multiple rank. In case all pair of variants are mutually compatible, we use the convex hull of all variants as an approximation to the set of all possible averages arising as observable laminated structures (Bhattacharya, 1993). For polycrystals containing large grains, for which more complicated microstructures are possible, our results can be interpreted as rigorous bounds on the overall energy.

As we said, we will consider two main examples, one in two dimensions and the other in three dimensions. In our two-dimensional example we will assume purely deviatoric transformation strains, for which the variants take the form

$$\varepsilon^{\mathrm{T}(1)} = \begin{bmatrix} a & 0 \\ 0 & -a \end{bmatrix} \quad \text{and} \quad \varepsilon^{\mathrm{T}(2)} = \begin{bmatrix} -a & 0 \\ 0 & a \end{bmatrix} \tag{1}$$

where a is a material constant. Our three-dimensional example, on the other hand, will assume orthorhombic variants (in which all pairs are mutually compatible) of the form

$$\varepsilon^{\mathrm{T}(1)} = \begin{bmatrix} \alpha & \delta & 0 \\ \delta & \alpha & 0 \\ 0 & 0 & \beta \end{bmatrix}, \quad \varepsilon^{\mathrm{T}(2)} = \begin{bmatrix} \alpha & -\delta & 0 \\ -\delta & \alpha & 0 \\ 0 & 0 & \beta \end{bmatrix}, \quad \varepsilon^{\mathrm{T}(3)} = \begin{bmatrix} \alpha & 0 & \delta \\ 0 & \beta & 0 \\ \delta & 0 & \alpha \end{bmatrix},$$

$$\varepsilon^{\mathrm{T}(4)} = \begin{bmatrix} \alpha & 0 & -\delta \\ 0 & \beta & 0 \\ -\delta & 0 & \alpha \end{bmatrix}, \quad \varepsilon^{\mathrm{T}(5)} = \begin{bmatrix} \beta & 0 & 0 \\ 0 & \alpha & \delta \\ 0 & \delta & \alpha \end{bmatrix},$$

$$\varepsilon^{\mathrm{T}(6)} = \begin{bmatrix} \beta & 0 & 0 \\ 0 & \alpha & -\delta \\ 0 & -\delta & \alpha \end{bmatrix} \tag{2}$$

where β, α, δ are material constants.

Our computations thus assume that the possible strains arising from phase transitions within a single grain are given by rotation — according to the crystallographic orientation of the grain — of the convex hull of the basic variants, which, in the cases we will consider are given by Eqs. (1) and (2). We will also assume isotropic stiffness

$$c_{ijkl} = \frac{2\nu}{1-2\nu}\mu\delta_{ij}\delta_{kl} + \mu\delta_{ik}\delta_{jl} + \mu\delta_{il}\delta_{jk}$$

with shear modulus μ and Poisson's ratio ν; and we will assume the elastic tensors

of both phases to be equal. If we denote by $R(x)$ the crystallographic orientation of the grain containing x, in accordance with our assumptions on the microstructure and texture, the set of admissible transformation strains is

$$\begin{aligned} S^{\mathrm{T}} &= \left\{\text{Statistically spatially homogeneous tensors } \varepsilon^{\mathrm{T}}\right\} \\ &= \varepsilon^{\mathrm{T}}(x) : R^{\mathrm{T}}(x)\varepsilon^{\mathrm{T}}(x)R(x) \text{ is a convex combination of the basic variants} \\ &\quad (1) \text{ or } (2). \end{aligned} \tag{3}$$

2.2. The effective energy

The numerical method presented here is based on a decomposition

$$W = W_1 + W_2 \tag{4}$$

of the overall elastic energy arising from an applied strain ε^0 and an admissible distribution of transformation strains $\varepsilon^{\mathrm{T}}(x)$, where

$$W_1 = \lim_{h\to 0} \frac{1}{2|\mathscr{P}|} \int_{\mathscr{P}} \sigma_{ij}^{(1)} \left[u_{i,j}^{(1)} - \varepsilon_{ij}^{\mathrm{T(av)}} \right] \tag{5}$$

and

$$W_2 = \lim_{h\to 0} \frac{1}{2|\mathscr{P}|} \int_{\mathscr{P}} \sigma_{ij}^{(2)} \left[u_{i,j}^{(2)} - \left(\varepsilon_{ij}^{\mathrm{T}} - \varepsilon_{ij}^{\mathrm{T(av)}} \right) \right]. \tag{6}$$

The limiting process $\lim_{h\to 0}$ in these equations corresponds to the small grain-size limit; (see Bruno and Goldsztein, 2000a for details). Further

$$\varepsilon^{\mathrm{T(av)}} = \lim_{h\to 0} \frac{1}{|\mathscr{P}|} \int_{\mathscr{P}} \varepsilon^{\mathrm{T}} \, \mathrm{d}x, \tag{7}$$

$u^{(1)}$ and $\sigma^{(1)}$ are given by

$$u_i^{(1)} = \varepsilon_{ij}^0 x_j, \tag{8}$$

$$\sigma_{ij}^{(1)} = c_{ijkl}\left(u_{k,l}^{(1)}, - \varepsilon_{k,l}^{\mathrm{T(av)}} \right); \tag{9}$$

the displacement $u^{(2)}$ is the solution of the equations of elasticity under the transformation strain

$$\begin{cases} \varepsilon^{\mathrm{T}}(x) - \varepsilon^{\mathrm{T(av)}} & \text{if } x \in \mathscr{P} \\ 0 & \text{otherwise} \end{cases}. \tag{10}$$

and vanishing boundary conditions at infinity, and $\sigma^{(2)}$ is the corresponding stress

$$\sigma_{ij}^{(2)} = \begin{cases} c_{ijkl}\left[u_{k,\,l}^{(2)} - \left(\varepsilon_{k,\,l}^{\mathrm{T}} - \varepsilon_{kl}^{\mathrm{T(av)}}\right)\right] & \text{if } x \in \mathscr{P} \\ c_{ijkl}u_{k,\,l}^{(2)} & \text{otherwise} \end{cases}. \tag{11}$$

The effective energy is the result of minimizing the elastic energy over all admissible transformation strains

$$\mathscr{E} = \min_{\varepsilon^{\mathrm{T}} \in \mathscr{S}^{\mathrm{T}}} W(\varepsilon^{\mathrm{T}}). \tag{12}$$

Our numerical method and upper bounds are based on explicit evaluations of the quantities W_1 and W_2. Algebraic expressions for these quantities can be obtained by direct evaluation of the expressions

$$W_1 = \frac{1}{2}c_{ijkl}\left(\varepsilon_{ij}^{0} - \varepsilon_{ij}^{\mathrm{T(av)}}\right)\left(\varepsilon_{kl}^{0} - \varepsilon_{kl}^{\mathrm{T(av)}}\right) \tag{13}$$

$$\begin{aligned} W_2 = {} & \frac{1}{2|\mathscr{P}|}c_{ijru}c_{tskl}\int_{\mathscr{P}}\left(\varepsilon_{ij}^{\mathrm{T}}(x) - \varepsilon_{ij}^{\mathrm{T(av)}}\right) \\ & \left\{\int_{\mathscr{P}}\Gamma_{rt,\,s}(x - x')\left(\varepsilon_{kl}^{\mathrm{T}}(x') - \varepsilon_{kl}^{\mathrm{T(av)}}\right)\mathrm{d}x'\right\}_{,u}\mathrm{d}x + \frac{1}{2|\mathscr{P}|}c_{ijkl} \\ & \int_{\mathscr{P}}\left(\varepsilon_{ij}^{\mathrm{T}}(x) - \varepsilon_{ij}^{\mathrm{T(av)}}\right)\left(\varepsilon_{kl}^{\mathrm{T}}(x) - \varepsilon_{kl}^{\mathrm{T(av)}}\right)\mathrm{d}x \end{aligned} \tag{14}$$

which follow from consideration of the Green's tensor Γ_{rt} and Eshelby integrals (Bruno and Goldsztein, 2000a).

3. Numerical method

While one can use the methods described here to evaluate the overall energy of general polycrystal, for simplicity we will restrict attention to polycrystals with a simplified grain structure in which (1) The crystallographic orientation of the grains is a random variable with uniform probability distribution, (2) The transformation strain is constant within each grain and it lies on the convex hull of the basic martensite variants, and (3) the d-dimensional polycrystal $\mathscr{P}(d = 2, 3)$ consists of a cubic array of $N = n^d$ cubic grains of the same size:

$$\mathscr{P} = \cup G = [0, 1]^d. \tag{15}$$

Here, calling $h = 1/n$, the grains G are of the form

$$G = G_{i_1,\ldots,i_d} = (i_1, \ldots, i_d)h + [0, h]^d \tag{16}$$

where i_j are integers satisfying $0 \le i_1, \ldots, i_d \le n - 1$.

For such a polycrystal the energy W_2 is given by

$$W_2 = \lim_{h\to 0} W_2^h$$

where, denoting by $\varepsilon^{\mathrm{T}}(G)$ the value of the transformation strain within the grain G, W_2^h is defined as

$$W_2 \approx W_2^h = \sum_{G,\, H\subseteq\mathscr{P}} \frac{1}{2|\mathscr{P}|} c_{ijru}c_{tskl}\left[\int_G \left\{\int_H \Gamma_{rt,\,s}(x-x')\,\mathrm{d}x'\right\}_{,u}\mathrm{d}x\right] \left(\varepsilon_{ij}^{\mathrm{T}}(G)-\varepsilon_{ij}^{\mathrm{T(av)}}\right)\left(\varepsilon_{kl}^{\mathrm{T}}(H)-\varepsilon_{kl}^{\mathrm{T(av)}}\right) + \sum_{G\subseteq\mathscr{P}} \frac{1}{2|\mathscr{P}|} c_{ijkl}|G|\left(\varepsilon_{ij}^{\mathrm{T}}(G)-\varepsilon_{ij}^{\mathrm{T(av)}}\right)\left(\varepsilon_{kl}^{\mathrm{T}}(G)-\varepsilon_{kl}^{\mathrm{T(av)}}\right). \tag{17}$$

Since the integrals in Eq. (17) can be computed analytically (Bruno and Goldsztein, 2000a, 2000b), W_2^h can be evaluated explicitly. More precisely, we have

$$W_2^h = \mu \sum_{G,\, H\subseteq\mathscr{P}} w_{ijkl}^{GH}\left(\varepsilon_{ij}^{\mathrm{T}}(G)-\varepsilon_{ij}^{\mathrm{T(av)}}\right)\left(\varepsilon_{kl}^{\mathrm{T}}(H)-\varepsilon_{kl}^{\mathrm{T(av)}}\right) \tag{18}$$

where w_{ijkl}^{GH} are explicit constants given by (Bruno and Goldsztein 2000a, 2000b).

We now introduce a sequence of approximations for the quantity W_2^h of Eq. (18) which, while maintaining accuracy, will allow us to reduce substantially the complexity of our minimization problem. These truncations depend on the statistics of the underlying field of crystallographic orientations. They are motivated by the analysis by Bruno et al. (1996) leading to upper bounds on the overall energy. More precisely, we approximate W_2 by $W_2^{h,\,r}$

$$W_2^h \approx W_2^{h,\,r} = \mu \sum_{\substack{G,\, H\subseteq\mathscr{P} \\ \mathrm{dist}(G,\,H)<r}} w_{ijkl}^{GH}\left(\varepsilon_{ij}^{\mathrm{T}}(G)-\varepsilon_{ij}^{\mathrm{T(av)}}\right)\left(\varepsilon_{kl}^{\mathrm{T}}(H)-\varepsilon_{kl}^{\mathrm{T(av)}}\right) \tag{19}$$

where $\mathrm{dist}(G,\ H)=\max\{|g_i - h_i|\}$ if $G=(g_1,\ldots,g_d)h+[0,\ h]^d$ and $H=(h_1,\ldots,h_d)h+[0,\,h]^d$ (Bruno and Goldsztein, 2000a, 2000b). We thus have,

$$W \approx W^{h,\,r} = W_1 + W_2^{h,\,r}. \tag{20}$$

Numerical evaluation of the effective energy (12) then results via solution of the minimization problem

$$\mathscr{E} \approx \mathscr{E}^{h,\,r} = \min\left\{W^{h,\,r}\left(\left[\varepsilon^{\mathrm{T}}(G)\right]\right): G\subseteq\mathscr{P}\right\}. \tag{21}$$

This is a quadratic programming problem for $[\varepsilon^{\mathrm{T}}(G)]$ since $W^{h,\,r}$ is a convex quadratic function and the set of admissible variables is a convex polygon. The

minimum indicated in Eq. (21) can be efficiently obtained through a rather simple minimization method, whose remarkable performance in our context can be understood as resulting from the fast decay of correlations. Our minimization algorithm proceeds as follows: given a grain G, the strain energy $W^{h,r}$ is minimized with respect to the transformation strain $\varepsilon^{\mathrm{T}}(G)$ while the rest of the transformation strains are held fixed. (Note that $\varepsilon^{\mathrm{T(av)}}$ varies in the process of minimization with respect to $\varepsilon^{\mathrm{T}}(G)$.) This defines the new state of the transformation strain $\varepsilon^{\mathrm{T}}(G)$, which is used in all subsequent calculations. Using a visiting schedule, the transformation strains of all the grains in the polycrystal are updated once per iteration. (Our computations use a lexicographic visiting schedule, but many other possibilities may be as efficient.) A (small) number of iterations of this process, finally, produces the minimum with the required accuracy. Our numerical computations are presented in Section 5 and we refer the reader to Bruno and Goldsztein (2000a and 2000b) for a detailed discussion of the complexity and convergence properties of our method.

4. Upper and lower bounds

In addition to numerical calculations it is valuable to consider rigorous upper and lower bounds for the energy, as they provide a degree of validation for the numerics, and they constitute a source of useful intuition on the problem. (In this regard we note, for example, that the numerical method we are presently proposing resulted as a generalization of the upper bounds of Bruno et al. (1996) and Smyshlyaev and Willis (1998)). Our derivation of lower bounds is based on a new method; our upper bound, on the other hand, generalizes the results of Bruno et al. (1996) and Smyshlyaev and Willis (1998) to the present non-rotationally-symmetric microgeometry.

4.1. Lower bound

Our derivation of lower bounds is based on partition of the polycrystal into a number of groups of grains. We thus divide the polycrystal $\mathscr{P}$ of Eq. (15) into groups containing $N_{\mathrm{g}} = n_{\mathrm{g}}^d$ grains. The total number of grains in the polycrystal may not be divisible by N_{g}, but we can always cover almost all of the polycrystal's body by using such groups. More specifically, we write

$$\mathscr{P} \supseteq \bigcup_{A \in \mathscr{A}} A \tag{22}$$

where, calling

$$A_{n_1,\ldots,n_d} = \bigcup_{i_1=n_1 n_{\mathrm{g}}}^{(n_1+1)n_{\mathrm{g}}-1} \cdots \bigcup_{i_d=n_d n_{\mathrm{g}}}^{(n_d+1)n_{\mathrm{g}}-1} G_{i_1,\ldots,i_d}, \tag{23}$$

we have set

$$\mathscr{A} = \left\{ \mathscr{A}_{n_1,\ldots,n_d} : 0 \le n_1, \ldots, n_d < \frac{n}{n_g} \right\}; \tag{24}$$

see Fig. 1 and Eq. (16).

From Eq. (6) and denoting, for $A \in \mathscr{A}$

$$W_A = \frac{1}{2|A|} \int_A \sigma_{ij}^{(2)} \left[u_{i,j}^{(2)} - \left(\varepsilon_{ij}^{\mathrm{T}} - \varepsilon_{ij}^{\mathrm{T(av)}} \right) \right], \tag{25}$$

we evidently have

$$W_2 \ge \sum_{A \in \mathscr{A}} |A| W_A. \tag{26}$$

Now, the quantities W_A themselves can be bounded from below by the energy of a corresponding traction free boundary value problem. Indeed, let $\tilde{v}$ be the solution of the equations

$$\tau_{ij,j} = 0$$

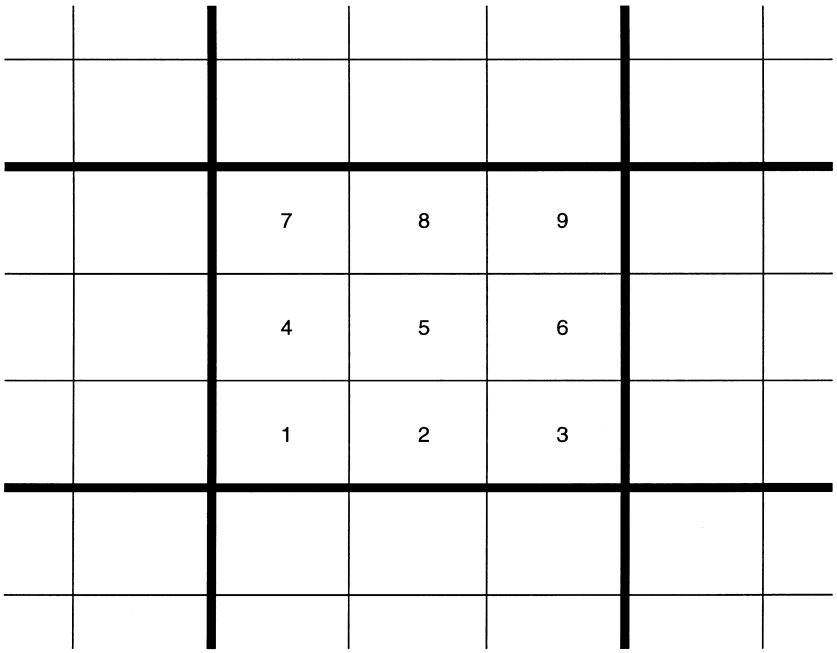

Fig. 1. A group of grains in the lower-bound decomposition of $\mathscr{P}$; $n_g = 3$ (two-dimensional example).

$$\tau_{ij} = c_{ijkl}\left[\tilde{v}_{k,\,l} - \left(\varepsilon^{\mathrm{T}}_{kl} - \varepsilon^{\mathrm{T(av)}}_{kl}\right)\right]$$

$$\tau_{ij}(x)\hat{n}_j(x) = 0, \quad x \in \partial A, \tag{27}$$

where $\tilde{n}$ is the normal to the boundary of A. Then, defining

$$F_A = \frac{1}{2|A|}\int_A \tau_{ij}\left[\tilde{v}_{i,\,j} - \left(\varepsilon^{\mathrm{T}}_{ij} - \varepsilon^{\mathrm{T(av)}}_{ij}\right)\right], \tag{28}$$

we have

$$W_A \geq F_A \tag{29}$$

since the solution of the traction free problem minimizes the corresponding energy integral. From Eqs. (26) and (29) we obtain the estimate

$$W = W_1 + W_2 \geq W_1 + \sum_{A\in\mathscr{A}} |A| F_A, \tag{30}$$

and thus

$$\mathscr{E} = \min_{\varepsilon^{\mathrm{T}}} W \geq \min_{\varepsilon^{\mathrm{T}}} \left\{ W_1 + \sum_{A\in\mathscr{A}} |A| F_A \right\}. \tag{31}$$

Clearly the quantity F_A depends on the array of crystallographic orientations as well as the distribution of transformation strains within the group A — which are the ones prescribed by the overall distributions in the polycrystal. Based on the convexity properties of F_A as a function of the transformation strains for fixed crystallographic orientation, the minimization of the right-hand side of Eq. (31) can be restricted to those distributions of transformation strains $\varepsilon^{\mathrm{T}}(x)$ which depend solely on the crystallographic orientations of the group A containing x. For example, in a two-dimensional configuration the crystallographic orientations of a group A are described by a vector $\vec{\theta}$ of angles, defining $\mathscr{L}$ by

$$\mathscr{L} = W_1 + \left(\frac{2}{\pi}\right)^{N_{\mathrm{g}}} \int_{\left[0,\frac{\pi}{2}\right]^{N_{\mathrm{g}}}} F\left(\varepsilon^{\mathrm{T}}(\vec{\theta}),\vec{\theta}\right) \mathrm{d}\theta_1,\ldots,\mathrm{d}\theta_{N_{\mathrm{g}}}, \tag{32}$$

we have (Bruno and Goldsztein, 2000a)

$$\mathscr{E} \geq L_1 = \min_{\varepsilon^{\mathrm{T}} = \varepsilon^{\mathrm{T}}(\vec{\theta})} \mathscr{L}. \tag{33}$$

The actual minimization indicated in Eq. (33) is quite cumbersome due to the constraints on the maximum size of the transformation strains. This calculation can be greatly simplified, however, by performing the minimization over the linear subspace of all strains obtained as arbitrary (non necessarily convex) linear

combinations of the admissible transformation strains. This leads to the rigorous, closed form lower bound L_1. This bound depends on singular multidimensional angular integrals which must be obtained numerically. The details of these numerical calculations are non-trivial and significant, (see Bruno and Goldsztein, 2000a). In the two-dimensional case they lead to our lower bound

$$L_1 = \frac{2\mu}{1-2\nu}\frac{1}{4}\left(\varepsilon_{11}^0+\varepsilon_{22}^0\right)^2+\mu\left(c_1\frac{1}{4}\left(\varepsilon_{11}^0-\varepsilon_{22}^0\right)^2+c_2\left(\varepsilon_{12}^0\right)^2\right); \tag{34}$$

the constants c_1 and c_2, which are closely related to the angular integrals mentioned above, were obtained in Bruno and Goldsztein (2000a). (As it is clear from our analysis, these constants depend on the number N_g of grains within each group, naturally the constants (and therefore the bounds) converge as the number N_g increases). Comparisons of the resulting lower bounds with an upper bound and numerical evaluations of the energy are given in the following section.

As mentioned above, closed form expressions have only been obtained from this general procedure through minimization over a subspace larger than the set of admissible transformation strains. As shown by (Bruno and Goldsztein, 2000a), for large values of the applied strains this procedure leads to poor estimates, and it is therefore advantageous to use an elementary lower bound in this regime. Such a bound can be obtained, quite simply, by neglecting the positive quantity W_2 in expression (4) prior to the minimization (12):

$$\mathscr{E} \geq \min_{\varepsilon^T \in \mathscr{S}^T} W_1. \tag{35}$$

(This bound is identical with the well known result which is obtained from relaxation of the constraint of compatibility between grains. Indeed, W_2 can be made to vanish by using appropriate discontinuous displacements.) In the two-dimensional case, for example, this procedure gives the elementary bound

$$\mathscr{E} \geq L_2 = \begin{cases} \dfrac{2\mu}{1-2\nu}(h^0)^2 & \text{if } 0 \leq d^0 \leq a\dfrac{2}{\pi} \\ \dfrac{2\mu}{1-2\nu}(h^0)^2+2\mu\left(d^0-a\dfrac{2}{\pi}\right)^2 & \text{if } d^0 \geq a\dfrac{2}{\pi} \end{cases}, \tag{36}$$

where

$$h^0 = \frac{1}{2}\left(\varepsilon_{11}^0+\varepsilon_{22}^0\right)$$

and

$$(d^0)^2 = \frac{1}{4}\left(\varepsilon_{11}^0-\varepsilon_{22}^0\right)^2+\left(\varepsilon_{12}^0\right)^2. \tag{37}$$

4.2. Upper bound

We obtain an upper bound U through minimization of the energy over an "uncorrelated" subset $\mathscr{T}$ of $\mathscr{S}^{\mathrm{T}}$, see Bruno et al. (1996). Our arguments follow Bruno et al. (1996) and Smyshlyaev and Willis (1998); the details of our calculations are not identical with the previous ones since the microgeometry we consider does not satisfy the hypothesis of circular symmetry of Smyshlyaev and Willis (1998). We will be brief and we refer the reader to Bruno and Goldsztein (2000a), Bruno et al. (1996), Smyshlyaev and Willis (1998) for a more detailed presentation.

Explicitly, we seek to minimize the energy over the set

$$\mathscr{T} = \{\varepsilon^{\mathrm{T}} \in \mathscr{S}^{\mathrm{T}} : \varepsilon^{\mathrm{T}}(x) \text{ depends only on the orientation of the grain containing } x\}, \tag{38}$$

see Eq. (3), so that our upper bound is

$$U = \min_{\varepsilon^{\mathrm{T}} \in \mathscr{T}} W. \tag{39}$$

For distributions in $\mathscr{T}$ the transformation strains in different grains are statistically independent, and thus

$$\left\langle \left(\varepsilon_{ij}^{\mathrm{T}}(G) - \varepsilon_{ij}^{\mathrm{T}(av)}\right)\left(\varepsilon_{kl}^{\mathrm{T}}(H) - \varepsilon_{kl}^{\mathrm{T}(\mathrm{av})}\right)\right\rangle = 0 \tag{40}$$

whenever $G \neq H$ (where we have used the notation $\langle f \rangle$ for the ensemble average of f). Since by ergodicity, the strain energy W does not depend on the particular realization under consideration, averaging over the ensemble of all possible realizations and minimizing over $\mathscr{T}$ yields

$$U = \min_{\varepsilon^{\mathrm{T}} \in \mathscr{T}} W = \min_{\varepsilon^{\mathrm{T}} \in \mathscr{T}} \langle W \rangle. \tag{41}$$

In view of Eqs. (18), (40) and (41) the upper bound U can be written in terms of single-grain integrals

$$U = \min_{\varepsilon^{\mathrm{T}} \in \mathscr{T}} \left\{ W_1 + \mu \sum_{G \subseteq \mathscr{P}} w_{ijkl}^{GG} \left(\varepsilon_{ij}^{\mathrm{T}}(G) - \varepsilon_{ij}^{\mathrm{T}(\mathrm{av})}\right)\left(\varepsilon_{kl}^{\mathrm{T}}(G) - \varepsilon_{kl}^{\mathrm{T}(\mathrm{av})}\right) \right\}. \tag{42}$$

Since this quantity depends on single grain energies only, it is possible to evaluate U in closed form. Explicit closed form expression for U (for two-dimensional examples) were given by Bruno et al. (1996), Smyshlyaev and Willis (1998) and, for our particular microgeometry, by Bruno and Goldsztein (2000a). Note that this upper bound U coincides with the approximation for the effective energy introduced in Section 3 when the interaction of any two different grains is

neglected (i.e. $r = 1$)

$$U = \lim_{h \to 0} \mathscr{E}^{h,\,1}.$$

Graphs comparing these bounds with numerical evaluations and lower bounds are presented in the following section.

4.3. Classical Taylor upper bound

As a reference for comparisons, we will also compute the classical Taylor bound (Taylor, 1938). This bound is the energy that would result if the elastic strain were everywhere equal to the applied strain ε^0. Thus, if a crystallite has orientation R with probability $p(R)$, the Taylor bound is given by

$$T = \sum_R \frac{c_{ijkl}}{2}\Big(\varepsilon^0_{ij} - \varepsilon^{\mathrm{T}}_{ij}(R)\Big)\big(\varepsilon^0_{kl} - \varepsilon^{\mathrm{T}}_{kl}(R)\big)p(R) \tag{43}$$

where $\varepsilon^{\mathrm{T}}(R)$ is the transformation strain that minimizes the energy of a crystal of orientation R, when the elastic strain is ε^0 throughout the crystal. The computation of this bound is given in Appendix A, and the results obtained are displayed in the next section.

5. Results

In this section, we present some of our numerical results and bounds for two- and three-dimensional polycrystals. We thus discuss the characteristics of the energy curves as functions of the applied strains (which seem specially interesting in the three-dimensional case). As it happens, numerical results and bounds are fully consistent with each other, and they demonstrate the robustness of our numerical approach.

In what follows we display various quantities related to the homogenized energy of polycrystals as a function of the magnitude ε of a deviatoric applied strain. We thus consider the computed values of the homogenized energy $\mathscr{E}$ itself, our upper and lower bounds U, and L, and, for reference, the Taylor bound T and the "Austenite Energy" E_{A}

$$E_{\mathrm{A}} = \frac{1}{2}c_{ijkl}\varepsilon^0_{ij}\varepsilon^0_{kl},$$

which equals the energy that would be required to deform the polycrystal in the absence of phase transitions. For definiteness (and following Bruno et al., 1996) we use the values $\mu = 100$ GPa and $\nu = 0.25$ for the elastic constants.

The size of the applied strain will be characterized by a parameter ε. Examples using deviatoric applied strains will be given both in the two- and three-dimensional case; in two dimensions we take applied strains of the form

$$\varepsilon^0 = \varepsilon \begin{bmatrix} 1 & 0 \\ 0 & -1 \end{bmatrix} \tag{44}$$

while, in the three dimensions we will use

$$\varepsilon^0 = \varepsilon \begin{bmatrix} -2 & 0 & 0 \\ 0 & 1 & 0 \\ 0 & 0 & 1 \end{bmatrix}. \tag{45}$$

The corresponding basic transformation strains (variants) are given by Eqs. (1) and (2) with $a = 0.02$ and, in the three-dimensional case,

$$\alpha = 0.0425, \quad \beta = -2\alpha, \quad \delta = 0.0194 \tag{46}$$

corresponding to γ_1' Cu-14Al-4Ni (see Otsuka and Shimizu, 1974).

The ranges of values of ε used for the graphs give applied deviators covering the interesting domain in which most of the phase transitions occur.

5.1. Two-dimensional examples

Let us consider the computed values for the homogenized energy $\mathscr{E} = \mathscr{E}(\varepsilon)$ in Fig. 2. This curve exhibits two main ranges of quadratic behavior, small ε and large ε, which are separated by an intermediate regime. More precisely, there is a constant c_e such that

$$\mathscr{E}(\varepsilon) \approx \mu c_e \varepsilon^2; \tag{47}$$

for ε small, and the second derivative of $\mathscr{E}(\varepsilon)$ approaches the limiting value 4μ as ε increases. We have obtained the value $c_e = 0.38$ from our numerics.

It is easy to understand the mechanisms leading to the domains of quadratic dependence. For small values of ε none of the grains transforms to a single variant but to a mixture. This is clearly demonstrated by the upper curves in Fig. 3, which show the volume fraction V occupied by the grains transformed to a single variant as a function of the applied strain. Within this regime both the strains and transformation strains depend linearly on ε since, as can be checked easily the elasticity problem is linear in ε as long as none of the grains in the polycrystal have transformed into a single variant. Linearity of the strains translates into quadratic behavior for the energy, as indicated in Eq. (47).

The bounds, also shown in Fig. 2, follow closely the numerical values of the effective energy. Like the homogenized energy, the bounds exhibit two main ranges of quadratic behavior, small ε and large ε, separated by an intermediate nonlinear regime. Our lower bound is given by

$$L(\varepsilon^0) = \max\{L_1(\varepsilon^0), L_2(\varepsilon^0)\}, \tag{48}$$

see Section 4 (The constants c_1 and c_2 in Eq. (34) depend on the number $N_g = n_g^2$ of grains within each group in our decomposition of the polycrystal; values for

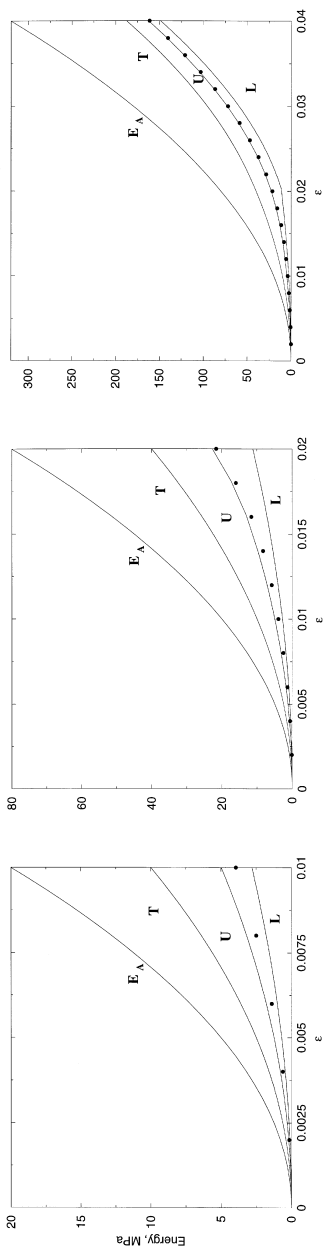

Fig. 2. Austenite energy E_A, Taylor bound T, upper bound U, lower bound L and effective energy $\mathscr{E}$ (in dotted line) as functions of the parameter ε of Eq. (44).

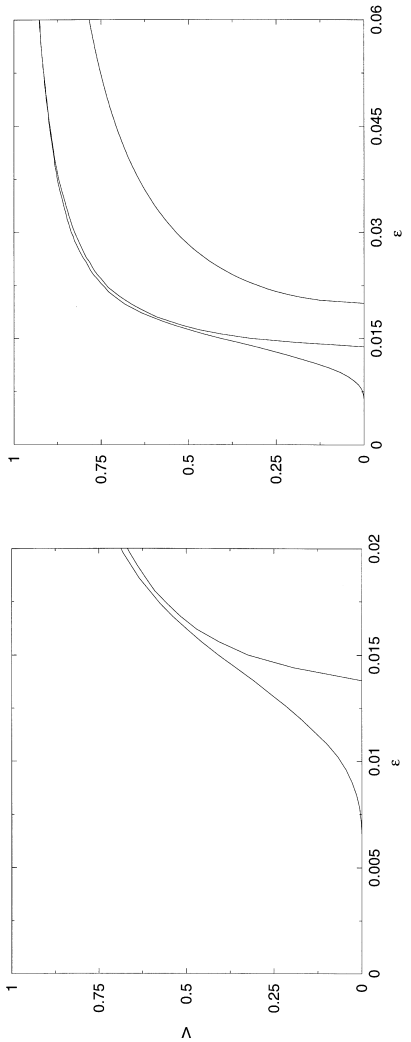

Fig. 3. Volume fraction V of grains transformed into a single variant as a function of ε. The upper curve is the result from the computations of the effective energy, the middle curve results from our upper bound and the lower curve from the Taylor bound.

these constants can be found by Bruno and Goldsztein (2000a). Naturally, larger values of N_g lead to sharper lower bounds on the energy.) As shown by Bruno and Goldsztein (2000a), on the other hand, the upper bound is given by the quadratic expression

$$U = \mu c_u \varepsilon^2 \quad \text{for } \varepsilon \leq \varepsilon^* \tag{49}$$

where $c_u = 0.4974$ and $\varepsilon^* = a \cdot 0.7047$. For large values of ε, finally, the curvature of the upper bound approaches that of the linear elastic material.

A deeper connection between $\mathscr{E}$ and its upper bound U emerges as we consider values of ε of the same order or larger than a. For such large values of ε, the grains transform to one of the variants and not to a mixture of them, and the choice of the one variant to be represented within any one grain depends mostly on the orientation of the grain. This implies that, in this regime, transformation strains from different grains are very nearly independent from each other (since the crystallographic orientations are independent) or, in other words, that the correlations between transformation strains of different grains are small. As a result, the minimizing distribution of transformation strains for the energy is quite close to the set of trial fields used in the derivation of the upper bound, and thus upper bound and homogenized energy agree very closely.

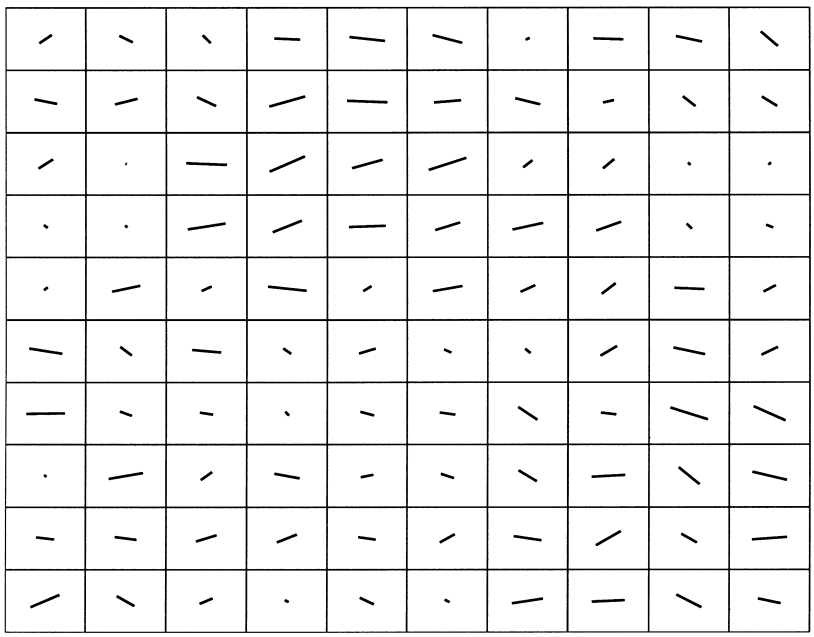

Fig. 4. Microstructure in a 10×10 portion of a 1000×1000 polycrystal transformed under $\varepsilon = 0.005$. Lines indicate grains orientations, with lengths proportional to the magnitude of the corresponding transformation strain.

It is of interest in this context to consider Fig. 4, which gives the crystallographic orientation and the transformation strains of a 10×10-grain window within our 1000×1000-grain polycrystal. Here, we have taken $\varepsilon = 0.005$; we see that most of the transformation occurs on favorably oriented crystallites.

5.2. Three-dimensional examples

Let us now consider our three-dimensional polycrystal. If we denote by $\varepsilon^{\mathrm{T}}(G)$ the transformation strain of the energy minimizing distribution in the grain G and by $R(G)$ the crystallographic orientation of the grain G, we have

$$\varepsilon^{\mathrm{T}}(G) = R(G)\left\{\sum_{i=1}^{6}\lambda_i(G)\varepsilon^{\mathrm{T}(i)}\right\}R^{\mathrm{T}}(G) \tag{50}$$

for some $\lambda_i(G)$ satisfying $\lambda_i(G) \geq 0$ and $\sum_{i=1}^{6}\lambda_i(G) = 1$. The fact that the basic variants $\{\varepsilon^{\mathrm{T}(i)}\}$ generate the space of the deviatoric strains, implies that for ε smaller than a critical threshold ε^*, ε^0 given by Eq. (45) can be written as convex combination of rotations of the basic variants by an arbitrary rotation (Bhattacharya and Kohn, 1996). In other words, ε^0 can be written in the form (50) for any grain G, and thus, the energy minimizing distribution of transformation strains is given by $\varepsilon^{\mathrm{T}}(G) = \varepsilon^0$ for all G (for which the elastic energy is 0). The value of ε^* has been calculated in Appendix A (see Eq. (A11). Figs. 5 and 6 show that for $0 \leq \varepsilon \leq \varepsilon^*$, the homogenized energy, our upper bound and the Taylor bound are exactly equal to zero. For $\varepsilon > \varepsilon^*$ the Taylor bound overestimates the energy by 50–250% (the larger percent error occurring for small departures from the zero energy set).

For $\varepsilon > \varepsilon^*$, not all the rotations R will have the property that ε^0 can be written as convex combination of $\{R\varepsilon^{\mathrm{T}(i)}R^{\mathrm{T}}\}$. In fact, for large enough values of ε none of the rotations will have this property. Thus, most of the grains G with crystallographic orientation for which ε^0 can not be written in the form (50), will transform to a transformation strain in the boundary of the convex hull of $\{R(G)\varepsilon^{\mathrm{T}(i)}R^{\mathrm{T}}(G)\}$ in the attempt to be close to ε^0 to minimize the energy. This implies that $\lambda_i(G) = 0$ for some i in Eq. (50). In fact, for any grain G, the number of $\lambda_i(G)$ which are equal to 0 in Eq. (50) increases with ε until eventually only one $\lambda_i(G)$ is equal to 1 and the rest of them are equal to 0 (i.e. the grain has transformed into a single variant). This behavior is illustrated in Figs. 7 and 8 where we have plotted the volume fraction of the grains for which k of the λ_i of Eq. (50) are different from 0 as a function of ε for $1 \leq k \leq 6$. As the number of $\lambda_i(G)$ which are equal to 0 increases, the grain G has less room to deform through phase transformation and thus, more elastic energy is required. As a consequence, the curvature of the energy curve increases (compare Figs. 7 and 8 with Figs. 5 and 6).

We now turn our attention to values of ε near ε^*. For $\varepsilon > \varepsilon^*$, these curves exhibit an asymptotic cubic behavior as $\varepsilon \to \varepsilon^*$. More precisely,

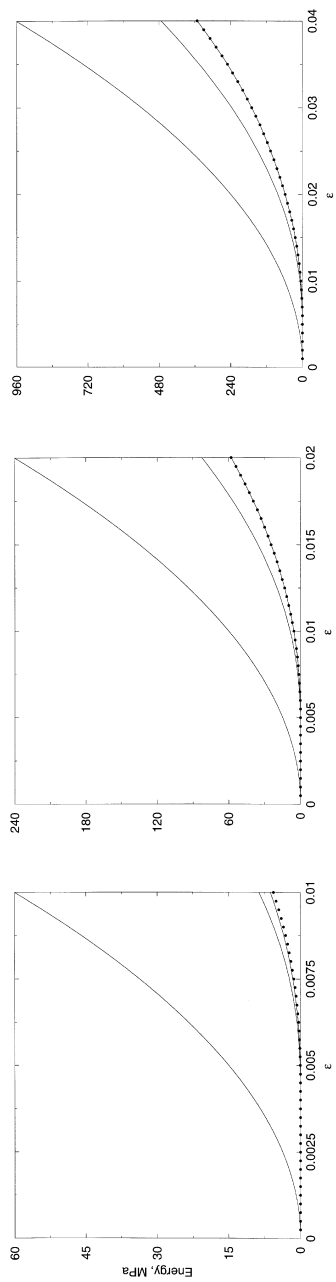

Fig. 5. In decreasing order Austenite energy E_A, Taylor bound T, upper bound U and effective energy $\mathscr{E}$ (in dotted line) as functions of ε. Note that in some cases the upper bound U is indistinguishable from the numerical results.

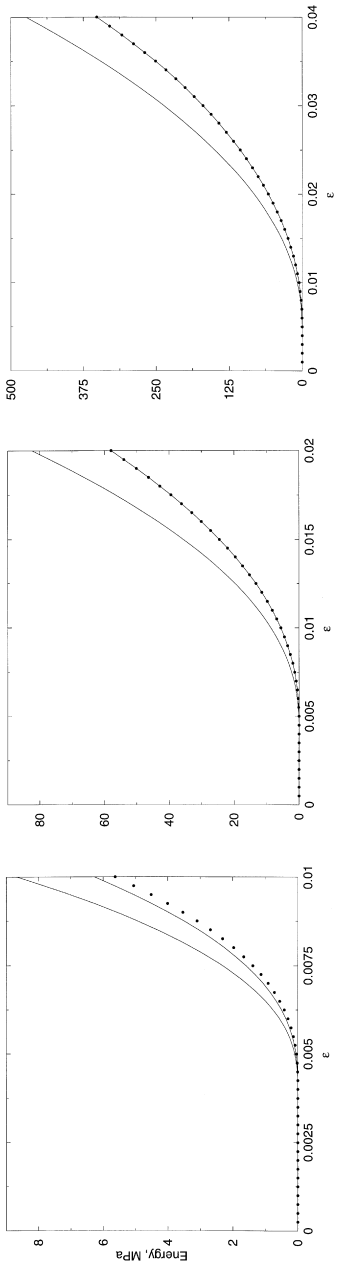

Fig. 6. Same as Fig. 5 except for the normalizing Austenite energy, which is not included here.

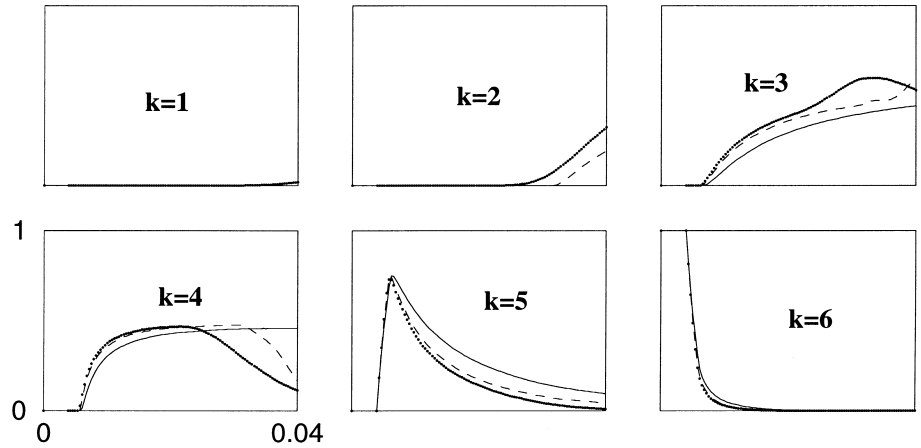

Fig. 7. Volume fraction of grains transformed into a convex combination of k variants as a function of ε. The dotted line corresponds to the computations of the effective energy, the dashed line was obtained with our upper bound and the solid line was obtained with the Taylor bound.

$$\mathscr{E}(\varepsilon) \approx E_0(\varepsilon - \varepsilon^*)^3 \quad \text{as } \varepsilon \to \varepsilon^*$$

$$U(\varepsilon) \approx U_0(\varepsilon - \varepsilon^*)^3 \quad \text{as } \varepsilon \to \varepsilon^*$$

$$T(\varepsilon) \approx T_0(\varepsilon - \varepsilon^*)^3 \quad \text{as } \varepsilon \to \varepsilon^*. \tag{51}$$

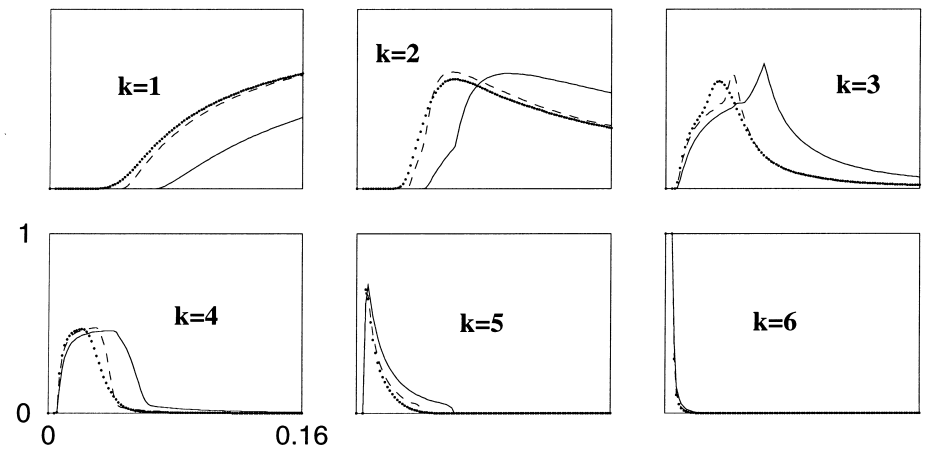

Fig. 8. Same as Fig. 7 for an expanded set of applied strains ε.

Table 1
Computed exponents in the asymptotic behavior of the effective energy and upper bound near ε^*

	$i = 0$	$i = 1$	$i = 2$	$i = 3$	$i = 4$	$i = 5$
e_i	2.51	2.75	2.89	2.95	2.99	3.00
u_i	2.46	2.66	2.80	2.89	2.95	2.98

Table 2
Computed prefactors (in 10^3 GPa) in the asymptotic behavior of the effective energy and upper bound near ε^*

	$i = 0$	$i = 1$	$i = 2$	$i = 3$	$i = 4$	$i = 5$
$E_0^{(i)}$	19	27	32	34	36	36
$U_0^{(i)}$	21	30	38	44	48	50

The asymptotic behavior of T and the calculation of T_0 have been obtained analytically in Appendix A (see Eqs. (A19) and (A20)). On the other hand, Eq. (51) for the effective energy has been obtained numerically as follows:

We first computed

$$\mathscr{E}_i = \mathscr{E}\left(\varepsilon^* + 0.01 \times 2^{-i}\right) \tag{52}$$

for $0 \le i \le 6$. If $\mathscr{E}$ has an asymptotic behavior of the form $\mathscr{E}(\varepsilon) \approx E_0(\varepsilon - \varepsilon^*)^e$, e can be approximated by

$$e \approx e_i = \frac{\log(\mathscr{E}_i/\mathscr{E}_{i+1})}{\log(2)}. \tag{53}$$

Table 1 clearly shows that e_i is very close to 3. Having obtained the exponent $e = 3$, E_0 has been approximated by

$$E_0 \approx E_0^{(i)} = \frac{\mathscr{E}_i}{(0.01 \times 2^{-i})^3}. \tag{54}$$

Table 2 contains the computed values of $E_0^{(i)}$. The asymptotic behavior of the upper bound was obtained similarly. More precisely, calling

$$U_i = U\left(\varepsilon^* + 0.01 \times 2^{-i}\right), \tag{55}$$

and assuming that $U \approx U_0(\varepsilon - \varepsilon^*)^u$, Table 1 contains

$$u \approx u_i = \frac{\log(U_i/U_{i+1})}{\log(2)}. \tag{56}$$

Analogously, Table 2 contains the approximations for U_0

$$U_0 \approx U_0^{(i)} = \frac{U_i}{(0.01 \times 2^{-i})^3}. \tag{57}$$

Acknowledgements

The authors gratefully acknowledge support from the NSF through Contract No. DMS-9523292. OB gratefully acknowledges support from NSF (through an NYI award and through Contracts DMS-9816802), from the AFOSR (through contracts No. F49620-96-1-0008 and F49620-99-1-0010) and from the Powell Research Foundation. Effort sponsored by the Air Force Office of Scientific Research, Air Force Materials Command, USAF, under grants number F49620-96-1-0008 and F49620-99-1-0010. The US Government is authorized to reproduce and distribute reprints for governmental purposes notwithstanding any copyright notation thereon. The views and conclusions contained herein are those of the authors and should not be interpreted as necessarily representing the official policies or endorsements, either expressed or implied, of the Air Force Office of Scientific Research or the US Government.

Appendix A. Taylor bounds

This appendix contains the derivations of the two- and three-dimensional Taylor bounds for applied strains of the form (44) and (45), respectively. Although, as shown in Section 5, the Taylor bounds lead to substantial overestimates of the energy, they do permit us to establish, without invoking numerical computations, the super-quadratic dependence of the overall energy discussed in Section 5.

A.1. Two-dimensional example

In our two-dimensional polycrystal, the possible transformation strains in a grain whose orientation is a rotation by an angle θ are given by

$$\varepsilon^{\mathrm{T}} = \lambda R \begin{bmatrix} a & 0 \\ 0 & -a \end{bmatrix}, \qquad R^{\mathrm{T}} = \lambda a \begin{bmatrix} \cos(2\theta) & \sin(2\theta) \\ \sin(2\theta) & -\cos(2\theta) \end{bmatrix}, \tag{A1}$$

where $-1 \le \lambda \le 1$. A simple calculation shows that the energy $W(\theta)$ of a crystal with orientation θ, transformation strain ε^{T} given by Eq. (A1) and applied strain ε^0 given by Eq. (44) is

$$W(\theta) = \frac{c_{ijkl}}{2}\left(\varepsilon_{ij}^0 - \varepsilon_{ij}^{\mathrm{T}}\right)\left(\varepsilon_{kl}^0 - \varepsilon_{kl}^{\mathrm{T}}\right) = 2a^2\mu\left(\lambda^2 - 2\varepsilon\lambda\cos(2\theta) + \varepsilon^2\right). \tag{A2}$$

Minimizing the above quantity over $-1 \le \lambda \le 1$ and taking average of the result over all orientations θ we obtain the Taylor bound

$$T = T(\varepsilon)\begin{cases} \mu\varepsilon^2 & \text{if } \varepsilon \le a \\ \mu\left(1 + \dfrac{4}{\pi}\theta_0 + \dfrac{\sin(4\theta_0)}{\pi}\right)\varepsilon^2 + \dfrac{8}{\pi}\mu(\theta_0 - \varepsilon\sin(2\theta_0)) & \text{otherwise} \end{cases}, \tag{A3}$$

where $0 \le \theta_0 < \pi/2$ is the solution of $\varepsilon\cos(2\theta_0) = a$.

A.2. Three-dimensional example

In our three-dimensional polycrystal, the possible transformation strains in a grain with orientation R are given by

$$\varepsilon^{\mathrm{T}} = R\left\{\sum_{i=1}^{6}\lambda_i\varepsilon^{\mathrm{T}(i)}\right\}R^{\mathrm{T}} \text{ with } \quad \lambda_i \ge 0 \text{ and } \sum_{i=1}^{6}\lambda_i = 1; \tag{A4}$$

where $\varepsilon^{\mathrm{T}(i)}$ are given by Eq. (2). The elastic energy W of a single crystal with constant transformation strain ε^{T} throughout the crystal under an applied strain ε^0 is

$$W = \frac{c_{ijkl}}{2}\left(\varepsilon^0_{ij} - \varepsilon^{\mathrm{T}}_{ij}\right)\left(\varepsilon^0_{kl} - \varepsilon^{\mathrm{T}}_{kl}\right). \tag{A5}$$

We are interested in computing the Taylor bound when the applied strain is given by Eq. (45). Thus, we first have to minimize the elastic energy W (Eq. (A5)) over the possible transformation strains given by Eq. (A4) with ε^0 of the form (45)

$$E = E(\varepsilon, R) = \min_{\varepsilon^{\mathrm{T}}}\left\{W : W \text{ is given by } (A5);\ \varepsilon^{\mathrm{T}} \text{ by } (A4) \text{ and } \varepsilon^0 \text{ by } (A5)\right\}, \tag{A6}$$

and then we need to take the average of the result over all possible orientations

$$T = T(\varepsilon) = \sum_{R} E(\varepsilon, R)p(R). \tag{A7}$$

In this last equation $p(R)$ is the probability that the orientation of any grain G is R, which in the examples considered here corresponds to the uniform probability distribution.

The minimization in Eq. (A6) is a quadratic programming problem. Unlike our two-dimensional example, we can not carry out this minimization explicitly. We thus solve Eq. (A6) numerically and then, perform the integration in Eq. (A7) also numerically. The resulting curve $T = T(\varepsilon)$ is displayed in Section 5.

A.2.1. Strains attainable with small Taylor energy

Since the basic variants in our three-dimensional example (see Eq. (2)) generate the space of deviatoric strains, there exists an ε^* such that $T(\varepsilon) = 0$ whenever $0 \le \varepsilon \le \varepsilon^*$ (Bhattacharya and Kohn, 1996). We will next compute ε^* and the asymptotic behavior of T when $\varepsilon - \varepsilon^*$ is positive and small.

A.2.1.1. Calculation of ε^*. It can be inferred immediately from Eqs. (A4)–(A7) that $T(\varepsilon)=0$ if and only if ε^0 can be written as convex combination of the rotated basic variants (2)

$$\varepsilon^0=\varepsilon\begin{bmatrix}-2 & 0 & 0\\ 0 & 1 & 0\\ 0 & 0 & 1\end{bmatrix}=R\left\{\sum_{i=1}^{6}\lambda_i\varepsilon^{\mathrm{T}(i)}\right\}R^{\mathrm{T}}$$
$$\text{with } \lambda_i=\lambda_i(R)\geq 0 \text{ and } \sum_{i=1}^{6}\lambda_i=1 \tag{A8}$$

for all rotations R. Solving Eq. (A8) for λ_i as functions of R and ε and denoting by n_i the $(1, i)$th component of R (i.e. $n_i=r_{1i}$), we find that

$$\lambda_1=\frac{\varepsilon}{6\alpha}(3n_3n_3-1)-\frac{3\varepsilon}{2\delta}n_1n_2+\frac{1}{6}$$

$$\lambda_2=\frac{\varepsilon}{6\alpha}(3n_3n_3-1)+\frac{3\varepsilon}{2\delta}n_1n_2+\frac{1}{6}$$

$$\lambda_3=\frac{\varepsilon}{6\alpha}(3n_2n_2-1)-\frac{3\varepsilon}{2\delta}n_1n_3+\frac{1}{6}$$

$$\lambda_4=\frac{\varepsilon}{6\alpha}(3n_2n_2-1)+\frac{3\varepsilon}{2\delta}n_1n_3+\frac{1}{6}$$

$$\lambda_5=\frac{\varepsilon}{6\alpha}(3n_1n_1-1)-\frac{3\varepsilon}{2\delta}n_2n_2+\frac{1}{6}$$

$$\lambda_6=\frac{\varepsilon}{6\alpha}(3n_1n_1-1)+\frac{3\varepsilon}{2\delta}n_2n_2+\frac{1}{6}. \tag{A9}$$

Thus $T(\varepsilon)=0$ if λ_i given by Eq. (A9) is positive for all i and all vectors $\hat{n}=(n_1, n_2, n_3)$ of norm 1 (i.e. $|\hat{n}|^2=n_1^2+n_2^2+n_3^2=1$).

Due to symmetry, it is enough to consider only one of the equalities in Eq. (A9) to compute ε^*. We choose the fifth equation. We thus regard λ_5 as a function of ε and $\hat{n}$ given by Eq. (A9), $\lambda_5=\lambda_5(\varepsilon, \hat{n})$. If ε is held fixed, λ_5 attains its minimum when

$$\hat{n}=\hat{n}^*=\left(0, \frac{1}{\sqrt{2}}, \frac{1}{\sqrt{2}}\right) \quad \text{and} \quad \hat{n}=-\hat{n}^*=\left(0, -\frac{1}{\sqrt{2}}, -\frac{1}{\sqrt{2}}\right). \tag{A10}$$

Since ε^* is the value of ε that makes this minimum equal to 0, solving $\lambda_5(\varepsilon^*, \hat{n}^*)=0$ we find that

$$\varepsilon^* = \frac{2\alpha\delta}{2\delta + 9\alpha} = 0.00391407548. \tag{A11}$$

A.2.1.2. Behavior of T near ε^*. We now turn to the study of the behavior of T near ε^*. We first note that

$$R^{\mathrm{T}} \begin{bmatrix} -2 & 0 & 0 \\ 0 & 1 & 0 \\ 0 & 0 & 1 \end{bmatrix} R = I - 3\hat{n} \otimes \hat{n} \tag{A12}$$

where $\hat{n}$ is the first row of the matrix R and $\hat{n} \otimes \hat{n}$ is the matrix that results from the tensor product of $\hat{n}$ with itself (i.e. $(\hat{n} \otimes \hat{n})_{ij} = n_i n_j$). As a consequence, it can be seen that E defined in Eq. (A6) depends only on ε and $\hat{n}$. We then write $E = E(\varepsilon, R) = E(\varepsilon, \hat{n})$. Given that we are considering the case in which the orientations are random variables with uniform probability distributions, we parametrize $\hat{n}$ by

$$\hat{n} = \hat{n}(\theta, \beta) = (\cos\theta \cos\beta, \sin\theta \cos\beta, \sin\beta) \tag{A13}$$

with $-\pi \le \theta < \pi$ and $-\frac{\pi}{2} \le \beta \le \frac{\pi}{2}$; and density probability distribution given by

$$f(\theta, \beta) = \frac{\cos\beta}{4\pi}. \tag{A14}$$

We thus also write $E = E(\varepsilon, \hat{n}) = E(\varepsilon, \theta, \beta)$. Analgously, we regard λ_i defined in Eq. (A9) as a function of ε, θ and β ($\lambda_i = \lambda_i(\varepsilon, \hat{n}) = \lambda_i(\varepsilon, \theta, \beta)$).

The first step in the evaluation of E is to define $\bar{\varepsilon} = \bar{\varepsilon}(\theta, \beta)$ as the maximum ε such that ε^0 is a convex combination of the rotated basic variants by a rotation R whose first row is $\hat{n}(\theta, \beta)$. This is equivalent to

$$\bar{\varepsilon}(\theta, \beta) = \max\{\varepsilon : \lambda_i(\varepsilon, \theta, \beta) \ge 0 \text{ for all } i\} \tag{A15}$$

(see Eq. (A9)). For example, noting that $\hat{n}^* = \hat{n}(\frac{\pi}{2}, \frac{\pi}{4})$ and recalling how we have obtained ε^*, we have $\bar{\varepsilon}(\frac{\pi}{2}, \frac{\pi}{4}) = \varepsilon^*$. In fact, for (θ, β) near $(\frac{\pi}{2}, \frac{\pi}{4})$, $\bar{\varepsilon}$ is given by the solution of the equation $\lambda_5(\varepsilon, \theta, \beta) = 0$. Thus, solving this last equation, expanding λ_5 around $(\varepsilon, \theta, \beta) = (\varepsilon^*, \frac{\pi}{2}, \frac{\pi}{4})$ we get

$$\bar{\varepsilon} = \bar{\varepsilon}(\theta, \beta) \approx \varepsilon^* + 9(\varepsilon^*)^2 \left\{ \frac{2\delta + 3\alpha}{12\alpha\delta} \left(\theta - \frac{\pi}{2}\right)^2 + \frac{1}{\delta}\left(\beta - \frac{\pi}{4}\right)^2 \right\} \quad \text{as} \quad (\theta, \beta) \to \left(\frac{\pi}{2}, \frac{\pi}{2}\right). \tag{A16}$$

Let us now compute $E(\varepsilon^* + \Delta, \theta, \beta)$ with Δ small and positive. We first note that $E(\varepsilon^* + \Delta, \theta, \beta) = 0$ whenever $\bar{\varepsilon}(\theta, \beta) \ge \varepsilon^* + \Delta$. Recall that $\lambda_5(\varepsilon^*, \hat{n}) = 0$ for two different vectors $\hat{n} = \hat{n}^*$ and $\hat{n} = -\hat{n}^*$ (see Eqs. (A9) and (A10)). Analogously, for each λ_i, there is a pair of vectors $\hat{n}(i)$ and $-\hat{n}(i)$ such that $\lambda_i(\varepsilon^*, \hat{n}) = 0$ if $\hat{n} = \hat{n}(i)$ or $\hat{n} = -\hat{n}(i)$. Since all these vectors are different, we conclude that there are 12

different pairs (θ_i, β_i) (one of them being $(\frac{\pi}{2}, \frac{\pi}{4})$) such that $\hat{\varepsilon}(\theta_i, \beta_i) = \varepsilon^*$. Thus, being Δ small, $\bar{\varepsilon}(\theta, \beta) \leq \varepsilon^* + \Delta$ will only be satisfied in the neighborhood of the points (θ_i, β_i) and as consequence $E(\varepsilon^* + \Delta, \theta, \beta)$ will only be different from 0 around those points. Given the symmetry of the present problem, we will concentrate our attention around the point $(\frac{\pi}{2}, \frac{\pi}{4})$.

It is not difficult to see that, if $\bar{\varepsilon}(\theta, \beta) \leq \varepsilon^* + \Delta$, the transformation strain $\varepsilon^{\mathrm{T}}(\theta, \beta)$ that minimizes the energy W in the evaluation of $E(\varepsilon^* + \Delta, \theta, \beta)$ (see Eq. (A6)) is a convex combination of $\{R\varepsilon^{\mathrm{T}(i)}R^{\mathrm{T}}\}$ with $0 \leq i \leq 6$ and $i \neq 5$. This last statement is equivalent to say that $\varepsilon^{\mathrm{T}}(\theta, \beta)$ is of the form

$$\varepsilon^{\mathrm{T}}(\theta, \beta) = \bar{\varepsilon}(\theta, \beta)\begin{bmatrix} -2 & 0 & 0 \\ 0 & 1 & 0 \\ 0 & 0 & 1 \end{bmatrix} + \sum_{i \neq 5} x_i R\varepsilon^{\mathrm{T}(i)}R^{\mathrm{T}} \tag{A17}$$

for some x_i satisfying $\sum x_i = 0$. Thus minimizing the elastic energy W (see Eq. (A5)) over the transformation strains of the form (A17) and using the approximation (A16) for $\bar{\varepsilon}(\theta, \beta)$ we obtain

$$E\big(\varepsilon^* + \Delta, \theta, \beta\big) \approx \begin{cases} 0 & \text{if } \bar{\varepsilon}(\theta, \beta) \geq \varepsilon^* + \Delta \\ 3\mu\left[2 - \dfrac{3(2\delta - 3\alpha)^2}{2\big(27\alpha^2 + 4\delta^2\big)}\right](\varepsilon^* + \Delta - \bar{\varepsilon}(\theta, \beta))^2 & \text{otherwise} \end{cases} \tag{A18}$$

We finally compute $T(\varepsilon^* + \Delta)$ by taking ensemble average of E given by Eq. (A18) and the multiplying the result by 12 (since, as mentioned above, we have focused our attention to only one of the 12 disjoint regions where $E \neq 0$) to get

$$T(\varepsilon^* + \Delta) = \int E\big(\varepsilon^* + \Delta, \theta, \beta\big) f(\theta, \beta)\, \mathrm{d}\theta\, \mathrm{d}\beta \approx T_0 \Delta^3 \tag{A19}$$

where

$$T_0 = \frac{\mu(2\delta + 9\alpha)^2}{\sqrt{6}\delta\alpha^{3/2}(2\delta + 3\alpha)^{1/2}}\left[1 - \frac{3(2\delta - 3\alpha)^2}{4\big(27\alpha^2 + 4\delta^2\big)}\right] = 9.2 \times 10^4 \text{ GPa}. \tag{A20}$$

References

Bhattacharya, K., 1993. Comparison of the geometrically nonlinear and linear theories of martensitic transformation. Continuum Mechanics and Thermodynamics 5, 205–242.

Bhattacharya, K., Kohn, R.V., 1996. Symmetry, texture and the recoverable strain of shape-memory polycrystals. Acta Materialia 44, 529–542.

Bruno, O.P., Goldsztein G.H., 2000a. A fast algorithm for the simulation of polycrystalline misfits:

martensitic transformations in two space dimensions. Proceedings of the Royal Society of London A, in press.

Bruno, O.P., Goldsztein, G.H., 2000b. A fast algorithm for the simulation of polycrystalline misfits: martensitic transformations in three space dimensions, in preparation.

Bruno, O.P., Reitich, F., Leo, P., 1996. The overall elastic energy of polycrystalline martensitic solids. Journal of Mechanics and Physics of Solids 44, 1051–1101.

Otsuka, K., Shimizu, K., 1974. Morphology and crystallography of thermoelastic Cu–Al–Ni martensite analyzed by the phenomenological theory. Transactions of the Japan Institute of Metals 15, 103–108.

Smyshlyaev, V.P., Willis, J.R. 1998. A 'non-local' variational approach to the elastic energy minimization of martensitic polycrystals. In: Proceedings of the Royal Society of London A, pp. 1573–1613.

Taylor, G.I., 1938. Plastic strain in metals. Journal of the Institute of Metals 62, 307–324.